TECHNICAL MEMORANDUM

640

Impact of a satellite-derived Leaf Area Index monthly climatology in a global Numerical Weather Prediction model

S. Boussetta, G. Balsamo, A. Beljaars, T. Kral[(1)], L. Jarlan[(2)]

Research Department

April 2011

(1) Czech Hydro-Meteorological Institute (CHMI), Prague, Czech Republic

(2) Centre d'Etudes Spatiales de la Biosphère (CESBIO), Meteo France, Toulouse, France and Direction de la Météorologie Nationale, Casablanca, Morocco

Also submitted to International Journal of Remote Sensing, Special issue on Recent Advances in Quantitative Remote Sensing

European Centre for Medium-Range Weather Forecasts
Europäisches Zentrum für mittelfristige Wettervorhersage
Centre européen pour les prévisions météorologiques à moyen

Series: ECMWF Technical Memoranda

A full list of ECMWF Publications can be found on our web site under:
http://www.ecmwf.int/publications/

Contact: library@ecmwf.int

European Centre for Medium Range Weather Forecasts
Shinfield Park, Reading, Berkshire RG2 9AX, England

The Leaf Area Index (LAI), defined as the one-sided green leaf area per unit ground area, is used in many Numerical Weather Prediction (NWP) models as an indicator of the vegetation development state which is of paramount importance to characterise land evaporation, photosynthesis and carbon uptake processes. The LAI is often simply represented by look-up tables, dependent on the vegetation type and seasons. However, global LAI datasets derived from remote sensing observations have more recently become available. These products are based on sensors such as the Advanced Very High Resolution Radiometer (AVHRR) or the Moderate Resolution Imaging Spectro-radiometer (MODIS), onboard polar orbiting satellites that can cover the entire globe within typically three days and with a spatial resolution of the order of 1 km. We examine the meteorological impact of satellite-derived LAI products on near-surface air temperature and humidity, which comes both from the leaves stomata transpiration and from the intercepted water on the leaves surface, re-evaporating into the atmosphere. Two distinct monthly LAI climatology datasets derived respectively from AVHRR and MODIS sensors are tested. A set of forecasts and data assimilation experiments with the Integrated Forecasting System of the European Centre for Medium-range Weather Forecasts is performed with the monthly LAI climatology datasets as opposed to a vegetation dependent constant LAI. The monthly LAI is shown to improve the forecasts of near-surface (screen-level) air temperature and relative humidity through its effect on evapotranspiration, with the largest impact obtained over needle-leaf forests, crops and grassland. At longer time-scales, the introduction of the monthly LAI is shown to have positive impact on the model climate particularly during the boreal spring where the LAI climatology has a large seasonal cycle.

1 Introduction

Land surface processes influence the partitioning of energy, mass and momentum fluxes between the land surface and the atmosphere which has been demonstrated by various numerical and experimental studies at different spatial and time scales (Sellers et al. 1996, Betts et al. 1996, Avissar and Liu 1996, Boussetta et al. 2008, Balsamo et al. 2009) and proven to bring significant skills in weather forecasting up to 6 weeks (e.g. Koster et al. 2009).

An accurate land surface model (LSM) is therefore essential in numerical weather prediction (NWP), and particularly for what concerns the vegetation layer. In fact, the vegetation contributes to the evaporation through the plant transpiration and direct evaporation of the plant-intercepted precipitation. In addition it affects the available surface energy through the radiative transfer process within the canopy (Deardorff 1978) modifying the surface albedo.

In most LSMs, the Leaf Area Index (LAI), defined as the one-sided green leaf area per unit ground area, is used as an indicator of the vegetation state (greening, mature, senescent, dormant). Traditionally, the LAI was represented through look-up tables dependant on the vegetation type (Viterbo and Beljaars 1995). Though its spatial variation was commonly specified according to the biome types, the LAI temporal variation was often neglected and sometimes climatological seasonality was introduced together with other major changes and the particular impact of the LAI seasonality could not be assessed (Dorman and Sellers 1989, Giard and Bazile 2000).

Following the advent of Advanced Very High Resolution Radiometer (AVHRR) observations onboard the National Oceanic and Atmospheric Administration (NOAA) satellite missions, quantitative spatial and temporal information on vegetation properties became available at the global scale. In fact, based on the Normalized Difference Vegetation Index (NDVI) observed by the AVHRR instrument several

algorithms were developed to retrieve the LAI information (Sellers et al. 1996, Los et al. 2000, Masson et al. 2003).

Later, other LAI products were extracted from the inversion of radiative transfer models based on the vegetation type and the atmospherically corrected surface reflectance. This is the case for the satellite radiances available from the Moderate Resolution Imaging Spectro-radiometer (MODIS) sensor onboard the Terra/Aqua satellites (Myneni et al. 2002), or from the VEGETATION onboard the SPOT-4 satellite (Baret et al. 2007). The usage of these products within LSMs was tested in a mesoscale NWP model (Knote et al. 2009) showing that more realistic LAI information is able to improve the short range forecast scores of lower-level variables but not their biases. Other studies focused on global circulation models (GCM) and the implication of introducing observed seasonally varying LAI on the simulations. These studies generally discussed the impact of LAI seasonal (Van den Hurk et al. 2003, Lawrence and Slingo 2004) and inter-annual (Guillevic et al. 2002) variability in terms of annual cycle of the hydrological fluxes. They showed that seasonal LAI can have a non-neligible impact on the seasonality of the surface evaporation and precipitation over land. The implication of this variability for the screen-level variables was not clear. Furthermore, the response of the model to different LAI observations was only investigated at the mesoscale (Knote et al. 2009).

In this paper, we examine the impact of introducing a monthly satellite-based LAI climatology on the near-surface air temperature and humidity by numerical experiments using the European Centre for Medium Weather Forecast (ECMWF) Integrated Forecasting system (IFS).

Currently the Hydrologically improved Tiled ECMWF Surface Scheme for Exchange over Land (HTESSEL; Balsamo et al. 2009) within the ECMWF IFS keeps all vegetation properties fixed in time, which is an oversimplified treatment of the vegetation layer and excludes any seasonal variation. In particular, the Leaf Area Index (LAI), which expresses the phenological phase of vegetation (growing, mature, senescent, dormant), is kept constant and assigned by a look-up table depending on the vegetation type, thus vegetation appears to be fully developed throughout the year. Using two distinct LAI monthly climatology datasets, based on MODIS observations (Jarlan et al. 2008) and on AVHRR observations (Masson et al. 2003), the impact of the LAI seasonal variability on the screen-level variables is assessed by comparing with a fixed LAI. Also the two observation based climatologies are compared through their impact on the screen-level variables. In this paper, section 2 illustrates how the vegetation layer is treated in HTESSEL focusing on the canopy transpiration and interception processes and the LAI within HTESSEL. Section 3 describes the observations based LAI climatologies showing their main features and discrepancies. Medium range forecasts, climate simulations and data assimilation experiments to assess the impact of LAI variability on the screen-level variables are described and discussed in section 4. Concluding remarks are given in section 5.

2 Parameterisation of the vegetation layer

For the computation of the surface energy balance, the Hydrology-Tiled ECMWF Surface Scheme (HTESSEL; Viterbo and Beljaars 1995, van den Hurk et al., 2000, Balsamo et al., 2009) is based on a subdivision of the grid box into 8 tiles: bare soil, high vegetation, low vegetation, high vegetation with snow beneath, snow on low vegetation, interception layer, sea-ice and open water.

The vegetation types are specified from the US Department of Agriculture Global Land Cover Climatology map (GLCC; Loveland et al. 2000; http://edcdaac.usgs.gov/glcc/glcc.html), which provides a 1 km resolution classification of 20 land surface types based on the Biosphere-Atmosphere Transfer Scheme (BATS; Dickinson et al. 1993).

The distinction between bare ground and vegetated coverage fractions is important for the evaporation processes. In the case of bare ground the water is evaporated from the topsoil layer only, while for the vegetated fraction the transpiration extracts the water from the entire soil column according to the root distribution in addition to evaporation from the interception reservoir.

The evapotranspiration process is parameterized via a canopy resistance in the following way:

$$E_i = \frac{\rho_a}{r_a + r_c}\left[q_L - q_{sat}\left(T_{sk,i}\right)\right] \tag{1}$$

where E_i is the evapotranspiration from vegetated tile i in the absence of snow and interception water, q_L is the humidity at the lowest model level, $q_{sat}\left(T_{sk,i}\right)$ is the saturated humidity for the vegetation skin temperature $T_{sk,i}$, r_a is the aerodynamic resistance and r_c is the canopy resistance formulated according to (Jarvis 1976):

$$r_c = \frac{r_{s,\mathbf{min}}}{LAI} f_1 f_2 f_3 \tag{2}$$

with $r_{s,\min}$ being the minimum stomatal resistance and f_1, f_2, f_3, three inhibition functions expressing respectively shortwave radiation deficit, soil moisture stress and atmospheric humidity deficit.

The evaporation from the interception reservoir is parameterized as follows:

$$E_i = \frac{\rho_a}{r_a}\left[q_L - q_{sat}\left(T_{sk,i}\right)\right] \tag{3}$$

The leaf area influences the evaporation through the wet fraction of the grid box c_1:

$$c_1 = \mathbf{min}\left(1, \frac{W_1}{W_{1m}}\right) \tag{4}$$

where W_{1m} is the maximum value of the intercepted water in the grid box defined as a function of the LAI:

$$W_{1m} = W_{1\max}[c_B + c_H.LAI_H + c_L.LAI_L] \tag{5}$$

$W_{1\max}$ is the maximum water on a single layer of leaves or bare ground set to 0.0002m, C_B is the fraction of the bare ground, C_H is the fraction of the high vegetation, C_L is the fraction of the low vegetation, LAI_H is the leaf area index of the high vegetation, LAI_L is the leaf area index of the low vegetation and W_1 is a prognostic variable defining the water contents in the interception reservoir:

$$\rho_w \frac{\partial W_1}{\partial t} = c_1 E_1 + D + I \tag{6}$$

where c_1E_1 is the evaporation from the interception reservoir, D the dew deposition and I is the fraction of precipitation collected by the interception reservoir.

Now, if we consider the evaporative fraction, Λ, defined as

$$\Lambda \equiv \frac{\lambda E}{H + \lambda E} \tag{7}$$

where H is the sensible heat flux and λ is the latent heat of vaporization, we can adapt the sensitivity equation of Λ to r_c used by Jacobs and De Bruin (1992) to LAI:

$$\frac{\partial \Lambda}{\partial r_c} = \frac{-\Lambda}{\left[1+\left(1+\frac{s}{\gamma}\right)\frac{r_a}{r_c}\right] r_c} \tag{8}$$

where s is the slope of the saturation specific humidity versus temperature curve and γ is the psychrometric constant.

This can be reformulated for LAI leading to:

$$\frac{\partial \Lambda}{\partial LAI}\frac{\partial LAI}{\partial r_c} = \frac{\partial \Lambda}{\partial LAI}\left(\frac{-LAI}{r_c}\right) = \frac{-\Lambda}{\left[1+\left(1+\frac{s}{\gamma}\right)\frac{r_a}{r_c}\right] r_c}, \tag{9}$$

$$\frac{\partial \Lambda}{\partial LAI} = \frac{\Lambda}{LAI}\frac{1}{\left[1+\left(1+\frac{s}{\gamma}\right)\frac{r_a}{r_c}\right]} \tag{10}$$

Equation (10) demonstrates the link between LAI and the screen-level variables through the energy partitioning. Following the above formulation, and given that the current HTESSEL model does not account for the LAI radiative shading which may affect the available energy for baresoil evaporation, an increase (decrease) of the LAI would generally result in increased (decreased) evaporation rates under a given atmospheric forcing. Both transpiration and canopy interception evaporation are contributing to the signal. Also, in the current HTESSEL model, there is no coupling of LAI and momentum flux. Roughness length is defined by a correspondence table dependent on vegetation type

regardless of its phenological development. The proposed modification consists of replacing an LAI that is fixed in time, by monthly LAI fields, derived from satellite based observations.

Table 1: HTESSEL vegetation types and parameters

Index	*Vegetation type*	*H/L*	C_{veg}	*LAI* ($m^2\ m^{-2}$)	$r_{s,min}$ (sm^{-1})
1	Crops, Mixed farming	L	0.90	3	180
2	short grass	L	0.85	2	110
3	Evergreen needleleaf trees	H	0.90	5	500
4	Deciduous needleleaf trees	H	0.90	5	500
5	Deciduous broadleaf trees	H	0.90	5	175
6	Evergreen broadleaf trees	H	0.99	6	240
7	Tall grass	L	0.70	2	100
8	Desert	-	0	0.5	250
9	Tundra	L	0.50	1	80
10	Irrigated crops	L	0.90	3	180
11	Semi-desert	L	0.10	0.5	150
12	Ice caps and glaciers	-	-	-	-
13	Bogs and marshes	L	0.60	4	240
14	Inland water	-	-	-	-
15	Ocean	-	-	-	-
16	Evergreen shrubs	L	0.50	3	225
17	Deciduous shrubs	L	0.50	1.5	225
18	Mixed forest/woodland	H	0.90	5	250
19	Interrupted forest	H	0.90	2.5	175
20	Water and land mixtures	L	0.60	4	150

2.1 Land-Cover and Leaf-Area-Index

Four climatological fields characterise the vegetation in HTESSEL. Two of them are the Land Cover index fields to indicate dominant high and low vegetation types (T_H, T_L; see Table 1) and the other two contain their fractional area coverage (A_H, A_L). Dominant high and low vegetation and bare soil areas are represented in each grid box by their respective coverage C_H, C_L and C_B. The vegetation coverage C_i of low and high types are the product of the area vegetation fraction A_i and a vegetation type-dependant density (or biome cover) $C_{veg}(T_i)$ (i being the subscript for high or low vegetation) characterizing the degree to which the foliage prevents shortwave radiation from reaching the ground as defined by Deardorff (1978), and the bare soil coverage is the residual fraction. In the absence of snow and interception which dynamically modifies the coverage fraction during the simulation, the expressions are as follows:

$$C_H = A_H C_{veg}(T_H)$$
$$C_L = A_L C_{veg}(T_L) \quad (11)$$
$$C_B = 1 - C_H - C_L$$

The LAI, the biome cover $C_{veg}(T_i)$ and the minimum stomatal resistance $r_{s,\,min}$ (all constants throughout the year) are extracted from look-up tables (Van den Hurk et al. 2000; see Table 1) according to the vegetation type map (GLCC).

For the sake of comparison with the other LAI datasets, we compute the total LAI value (LAI_T) within a grid box, as a coverage weighted average of high and low vegetation LAI (see figure 1 for HTESSEL):

$$LAI_T = C_H LAI_H + C_L LAI_L \quad (12)$$

Table 2: Vegetation types and corresponding biome cover in ECOCLIMAP

Index	*Vegetation type*	*H/L*	C_{veg}
1	Deciduous forest	H	0.95
2	Coniferous forest	H	0.99
3	Rain forest	H	0.99
4	C3 Grass	L	$1\text{-}e^{-0.6\,LAI}$
5	C4 Grass	L	$1\text{-}e^{-0.6\,LAI}$
6	C3 Crops	L	$1\text{-}e^{-0.6\,LAI}$
7	C4 Crops	L	$1\text{-}e^{-0.6\,LAI}$

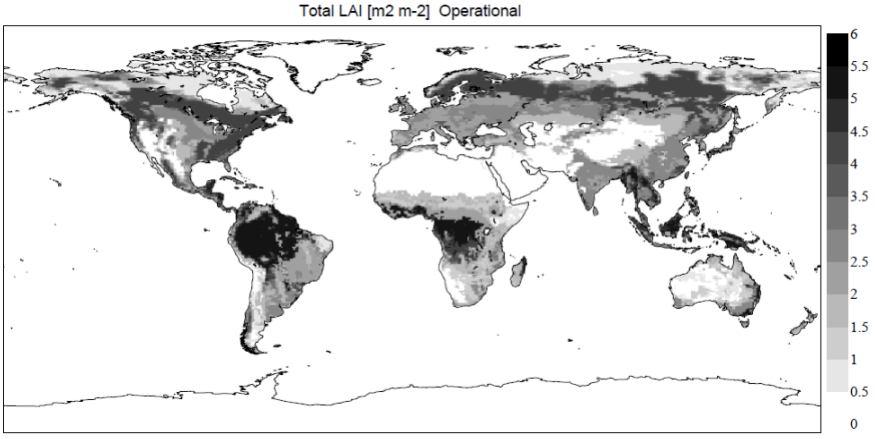

Figure 1:Total LAI [m^2m^{-2}] as defined in the operational system

3 The LAI datasets

3.1 AVHRR-based LAI from ECOCLIMAP

ECOCLIMAP is a global surface database providing high resolution (1-km) surface parameters needed for running land surface schemes (LSMs) in GCMs (Masson et al. 2003). Albedo, surface emissivity, soil texture, surface roughness, fraction of soil cover, minimum stomatal resistance and LAI are available.

For its derivation, four products are used: a derived land cover map, the Koeppe climate classification map, the FAO soil texture map (as in HTESSEL) and a one year (1992-1993) Normalized Difference Vegetation Index (NDVI) product derived from the Advanced Very High Resolution Radiometer (AVHRR) observations. First using the land cover map and the NDVI time series, an ecosystem classification map is derived, and then using look-up tables, surface parameters are assigned to each pixel of the ecosystem map.

The derivation of the LAI is based on a linear combination of the minimum and maximum values of the NDVI from the one year AVHRR time series together with minimum and maximum LAI values by ecosystems derived from the literature:

$$LAI = LAI_{\min} + \frac{\left(NDVI - NDVI_{\min}\right)}{\left(NDVI_{\max} - NDVI_{\min}\right)} \times \left(LAI_{\max} - LAI_{\min}\right) \tag{13}$$

In this analysis, the ECOCLIMAP vegetation covers (C_H, C_L and C_B) are derived in a similar way as in the case of the operational map based on a vegetation type dependant density $C_{veg}(T_i)$ and the area vegetation fraction A_i (equations 11). For the low vegetation types $C_{veg}(T_i)$ is expressed with a functional dependency from LAI following Kanemasu et al. (1977). This product is referenced as ECOCLIMAP LAI in the following sections.

3.2 MODIS LAI collection 5

The Moderate Resolution Imaging Spectroradiometer (MODIS) instrument is operating on both the Terra and Aqua satellites. It has a viewing swath width of 2330 km and covers the entire surface of the Earth every one to two days. Its detectors measure 36 spectral bands between 0.405 and 14.385 µm, and it acquires data at three spatial resolutions: 250m, 500m, and 1000m.

The FPAR (the Fraction of absorbed Photosynthetically Active Radiation) and LAI MODIS products (MOD15A2, used here) are derived from the MODIS sensor on board of TERRA. Both of these variables are produced daily at 1 km spatial resolution from MODIS spectral reflectance with a global coverage for all vegetated land surfaces, then synthesized on an 8-days time interval based on the maximum FPAR in order to remove the atmospheric noise (Myneni et al. 2002).

The MODIS LAI Level 4 algorithm consists of the inversion of a 3D radiative transfer model that computes the LAI and FPAR based on the biome type and an atmospherically corrected surface reflectance. Should this main algorithm fail, a back-up algorithm is triggered to estimate LAI and FPAR from empirical relationships with vegetation indices (Knyazikhin et al. 1998). The algorithm uses a land cover classification that is compatible with the radiative transfer model used in their derivation.

In this work, the collection 5 (released in 2008) of this product, available from February 2000 to present, has been used. This collection relies on a new land cover classification based on an 8-biomes map (grasses and cereal crops, shrubs, broadleaf crops, savannas, deciduous broadleaf forests, evergreen broadleaf forests, deciduous needleleaf forests and evergreen needleleaf forests). In these products, the LAI is defined as the biomass equivalent of FPAR, expressed as a dimensionless ratio of leaf area covering a unit of ground area (m^2 m^{-2}).

To derive the climatological time series, 9 years of data (2000-2008) were re-projected from the sinusoidal to a geographic regular lat/lon projection, spatially averaged to 1/12th deg resolution, then temporally smoothed, monthly averaged (Jarlan et al. 2008) and finally interpolated to a reduced Gaussian grid.

3.3 Mapping and comparing LAI

Both the ECOCLIMAP and MODIS LAI products were analysed and validated in previous studies (Carrigues et al. 2008, MODIS Land team http://landval.gsfc.nasa.gov/). Compared to ECOCLIMAP, which is based on one year (1992-1993) satellite observations only, this MODIS climatology based on a 9-year averaging process (2000-2008), has the advantage of being more robust. In order to be used in the HTESSEL scheme, this climatology should match the high and low vegetation concept and therefore, the total derived LAI should be split into a high and a low vegetation component. To do so, assuming a perfect land cover map, we rescale the total MODIS LAI with the operational one:

$$\Delta LAI = LAI_{MODIS} - LAI_{Operational},$$

$$LAI_{H,MODIS} = LAI_{H,Operational} + C_H \Delta LAI, \tag{14}$$

$$LAI_{L,MODIS} = LAI_{L,Operational} + C_L \Delta LAI,$$

where C_H and C_L are the high and low vegetation cover respectively.

The ECMWF operational LAI is constant throughout the year, however a map is generated following eq. 12. This is compared with ECOCLIMAP and MODIS LAI for the months of January and July which correspond roughly to the minimum and maximum LAI periods of the year for the northern hemisphere.

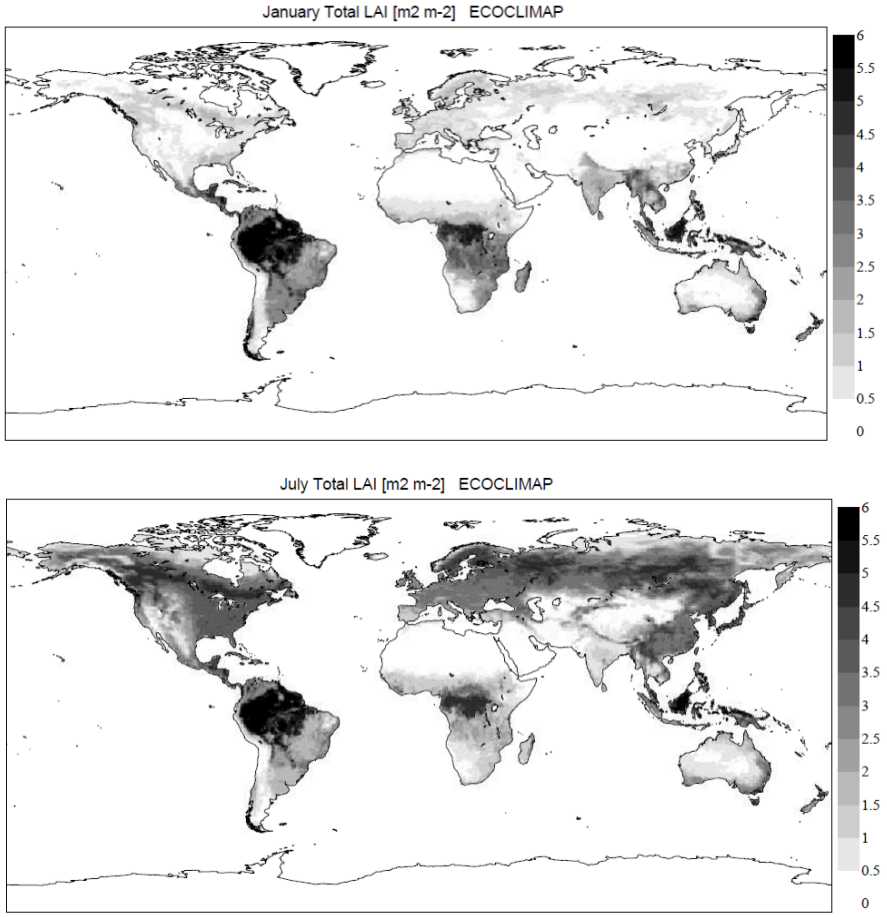

Figure 2: Total LAI [m^2m^{-2}] from ECOCLIMAP for January (upper) and July (lower)

For the July values of ECOCLIMAP and MODIS (the lower panels of figures 2 and 3 respectively) the global main spatial features of the LAI, generally agree with each other and with the operational map (figure 1), as the signatures of the African tropical forest, the Amazon area, the Boreal forest and the North-East European forest as well as the signature of crop areas like central Europe and western USA are correctly captured by the three datasets. Nevertheless, the magnitude and the spatial extent of these signatures can vary significantly by regions.

On the other hand, when looking at the differences between January and July values, we can see the large seasonal variability expressed in ECOCLIMAP (figure 2) and MODIS (figure 3) products especially in the northern hemisphere and obviously neglected in the ECMWF map (figure 1). This variability is even more pronounced in the Boreal and the Russian forests where an LAI difference of 5 can be reached between July and January suggesting that these products lack LAI for evergreen forest during northern-hemisphere winter.

Figure 4 shows the zonal averages of the maximum and minimum LAI.

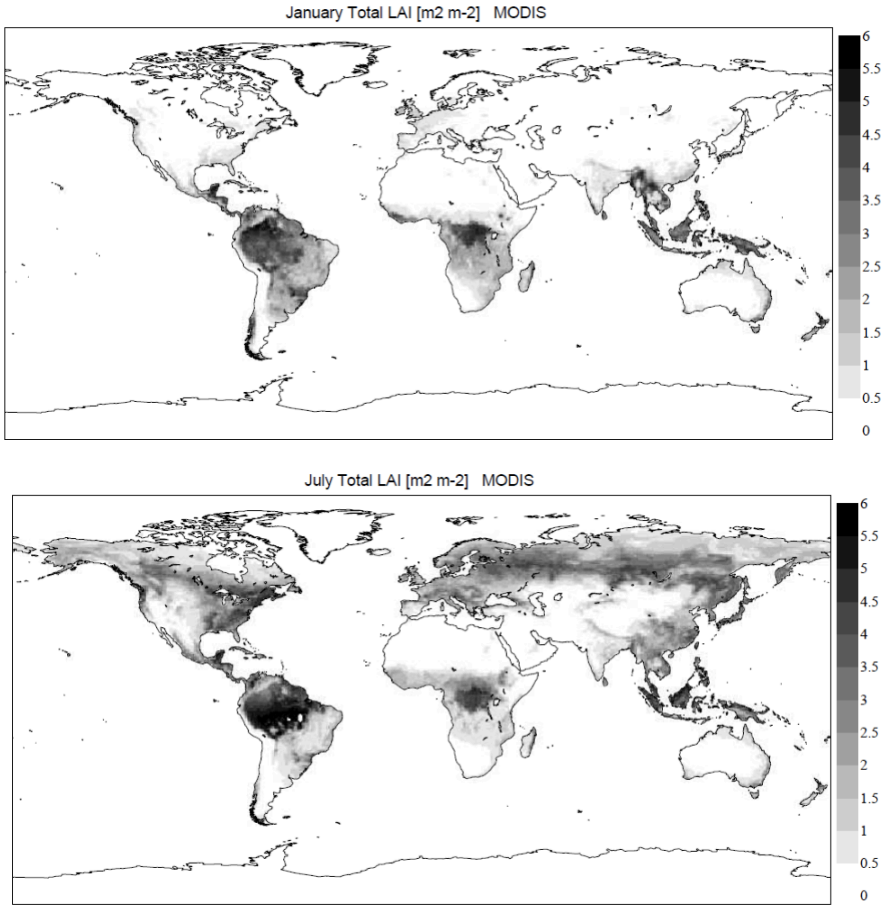

Figure 3: Total LAI[m^2m^{-2}] from MODIS climatology for January (upper) and July (lower)

Similarly to the previous figures, the three datasets express well the latitudinal variability in general. Compared to ECOCLIMAP and the ECMWF operational map, MODIS LAI magnitude is generally smaller. Among the commonly stated reasons for this lower amplitude of the MODIS LAI, is the reflectance saturation of the satellite observation for dense canopies (Myneni et al. 2002), this is not the case for ECOCLIMAP since it relies not only on the satellite observation but also on maximum and minimum values from look-up tables (eq. 13). This lower amplitude of the MODIS LAI is even bigger for the non dense canopy (minimum values) indicating that reflectance saturation can not be the only reason. At high latitude, snow can also affect the satellite observations, and may be the reason for the low LAI magnitude in MODIS. Also, the maximum values, in spite of showing a similar pattern for the three datasets, a 10% to 30% difference are seen especially at high latitudes. These discrepancies are also attributed to the differences in sensors and retrievals algorithms between ECOCLIMAP (AVHRR) and MODIS products. Another common reason for discrepancies is the difference in biome definition for some areas. However Lotsch et al. (2003), have stated that disagreement in land cover maps do not translate into strong disagreement in LAI estimates.

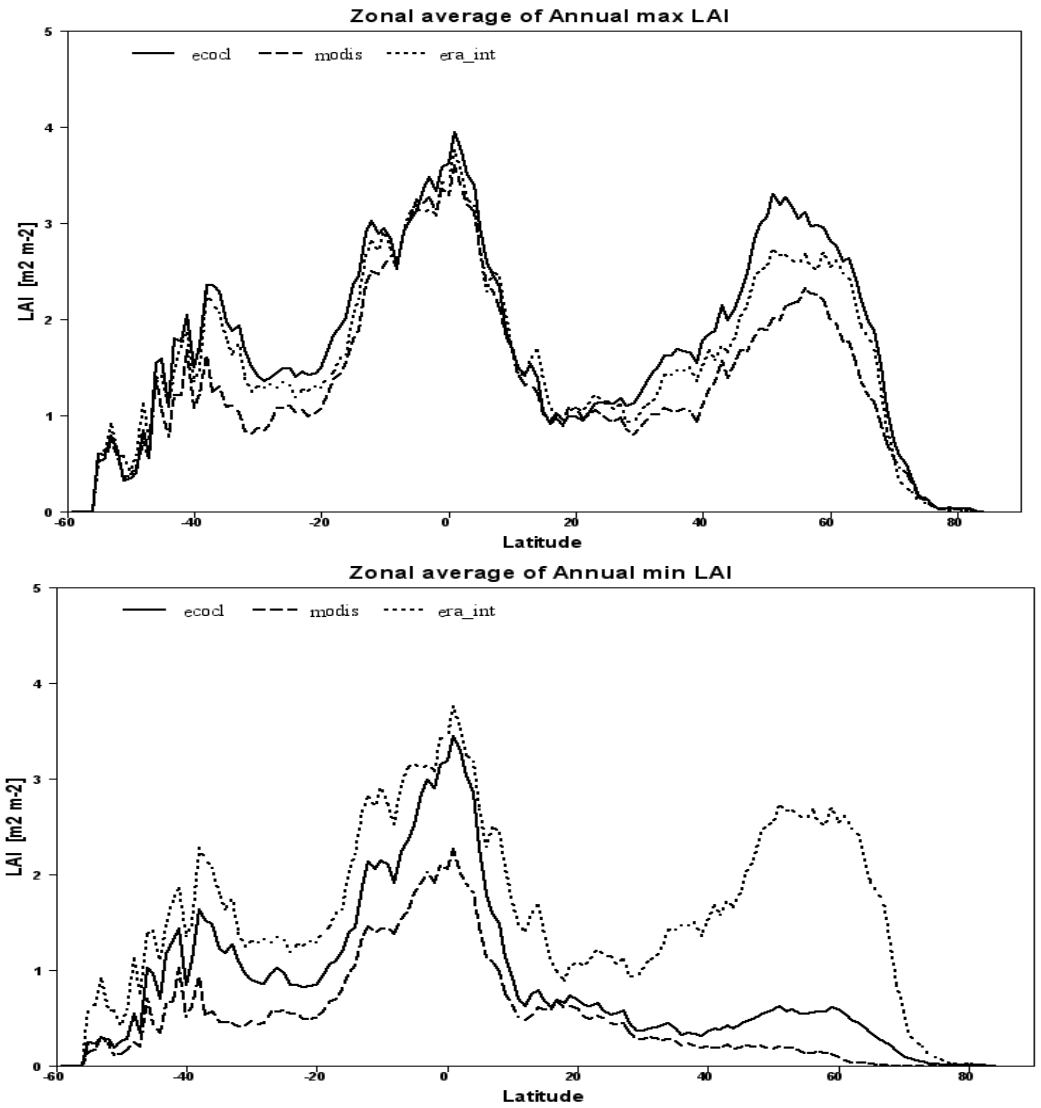

Figure 4: Zonal average of annual maximum LAI [m^2m^{-2}] (upper) and minimum LAI (lower) from the operational look-up table (dotted), ECOCLIMAP (solid) and MODIS (dashed)

Given the role of LAI in the evaporation formulation, it is expected that its seasonal cycle would play an important role and have particularly an impact on the prediction of the near surface temperature and humidity. The differences between the two considered LAI datasets are sometimes large and a direct comparison is beyond the scope of this paper. However an attempt is made to assess the relative merit of the two datasets by evaluating their meteorological impact on temperature and humidity forecasts.

4 Results

In order to evaluate the impact of the seasonally varying LAI on the surface-atmosphere interaction, the IFS coupled to the surface scheme HTESSEL was used. The default setting of the vegetation parameters in the operational IFS-HTESSEL is described in section 2 (Table 1), and has no seasonal variation. The model with this vegetation setting is used as a reference (control).

The simulations consisted of three types of model integrations:

Forecast experiments. In these experiments, medium range forecasts are run with the updated model version (i.e. with seasonally varying LAI) from existing operational analyses as initial condition.

Data assimilation experiments. In these experiments, both analyses and forecasts are run with the same model version. The interaction of the seasonal LAI and evaporation with the soil moisture analysis is particularly relevant, as the new model version may change the soil moisture increments. These experiments are also used for verification of the surface energy budget at a forest flux tower site and to illustrate the impact of the LAI revision on net radiation and sensible and latent heat fluxes.

Long integration experiments. These experiments are meant to assess the impact of the seasonally varying LAI on the climate of the model, particularly its seasonal cycle.

The details of the experiments are described in table 3. In all experiments, special emphasis is put on the evaluation of the 2m temperature and humidity, as they are directly affected by changes in the partitioning of energy at surface into sensible and latent heat flux.

Table 3: Experiments used for the LAI seasonality impact assessment

Experiment type	Experiment code	Period	Cycle	Resolution	Description
Forecast	f7wx	20080101-20090101	35r3	T399	Control (original LAI)
	f7vr	20080101-20090101	35r3	T399	LAI from ECOCLIMAP
	f87n	20080101-20090101	35r3	T399	LAI from MODIS
	f8mu	20080101-20090101	35r3	T399	LAI from MODIS+ minimum stomatal resistance adjustment
Assimilation	f85e	20080214-20080901	35r3	T255	Control (original LAI)
	f85f	20080214-20080901	35r3	T255	LAI from ECOCLIMAP
	f8o5	20080214-20080901	35r3	T255	LAI from MODIS+ minimum stomatal resistance adjustment
Climate	f8lb	20000801-20010930	36r1	T159	Control (original LAI)
	f9z0	20000801-20010930	36r1	T159	LAI from MODIS+ minimum stomatal resistance adjustment

4.1 Forecast experiments

A series of 37 10-days forecast lagged by 10 days starting on 1st January 2008 00UTC and ending on 1st January 2009 00UTC was performed using the different LAI climatologies. The control one (Ctl

LAI), has the annual constant LAI (table 1) whereas experiments ECO_LAI and MODIS_LAI use monthly climatology from ECOCLIMAP and MODIS respectively.

Here we focus on the short range forecasts (mainly 36 hours) which have the advantage that the synoptic situation is very close to reality. However changes in LAI will have impact on near surface temperature and humidity through sensible and latent heat flux. Screen-Level temperature and moisture can be verified using the analysis, which draws closely to the SYNOP observations. The model is run with 91 vertical levels at T399 (~50 km) horizontal resolution.

The assessment of the seasonal LAI impact was done for the screen-level temperature and relative humidity through 2 statistics named hereafter sensitivity and impact:

$$Sensitivity(T) = T_{MLAI} - T_{ctl} \tag{15}$$

$$Impact(T) = \left|T_{ctl} - T_{an}\right| - \left|T_{MLAI} - T_{an}\right| \tag{16}$$

Where subscripts *MLAI* refer to monthly LAI (ECO_LAI or MODIS_LAI) and "*an*" refer to the operational analysis. The equivalent quantities are computed for relative humidity. Therefore a positive (negative) sensitivity would mean an increase (decrease) of temperature/relative humidity at the 2m level due to introduction of the seasonal LAI. A positive (negative) impact means a reduction (increase) of the 2m temperature/relative humidity bias in comparison to the operational analysis due to introduction of the seasonal LAI.

Tables 4 and 5 show respectively the results for ECO_LAI and MODIS_LAI experiments for the global land at the FC+36h range (valid at 12UTC) in comparison to the control run for the 4 seasons. Both experiments show that by introducing the seasonal LAI, the 2 m temperature tends to increase while the relative humidity tends to decrease resulting in a positive impact on the temperature and a slight negative impact on relative humidity. This sensitivity is consistent with the LAI maps as seen in section 3.4 since the Ctl LAI (set to a maximum value throughout the year) is in average bigger than the introduced observed ones. Figure 5 and 6 displays the MAM spatial variability of impact and sensitivity of introducing MODIS LAI relative to the control run for temperature and relative humidity, respectively. The biggest impact is obviously seen during the transition season MAM especially above locations where the seasonal cycle of the vegetation is marked (northern latitudes, tropical Africa) as the evapotranspiration starts to be active while the seasonal LAI is still small compared to the Ctl LAI.

Table 4: Sensitivity and impact for 2m temperature [K] and relative humidity [%] globally over land at FC+36 (valid 12UTC) for the different forecast experiments

Experiment	season	T_sensitivity	T_impact	RH_sensitivity	RH_impact
ECOCLIMAP LAI vs CTL	DJF	0.11	0.003	-0.776	-0.28
	MAM	0.167	0.026	-1.08	-0.069
	JJA	0.087	0.003	-0.465	-0.146
	SON	0.104	0.019	-0.874	-0.202
MODIS LAI vs CTL	DJF	0.127	0.006	-0.965	-0.25
	MAM	0.185	0.035	-1.381	-0.023
	JJA	0.176	0.014	-1.202	-0.288
	SON	0.151	0.026	-1.347	-0.288
MODIS LAI vs ECOCLIMAP	DJF	0.017	0.003	-0.189	0.03
	MAM	0.018	0.009	-0.301	0.045
	JJA	0.09	0.011	-0.737	-0.142
	SON	0.047	0.007	-0.472	-0.086

Comparing the results from the two experiments based on the seasonal LAI (ECO_LAI and MODIS_LAI) shows that using the MODIS LAI climatology has a better impact on the 2m temperature for all the seasons while for the relative humidity the impact is positive for DJF and MAM and negative for the other seasons (table 4).

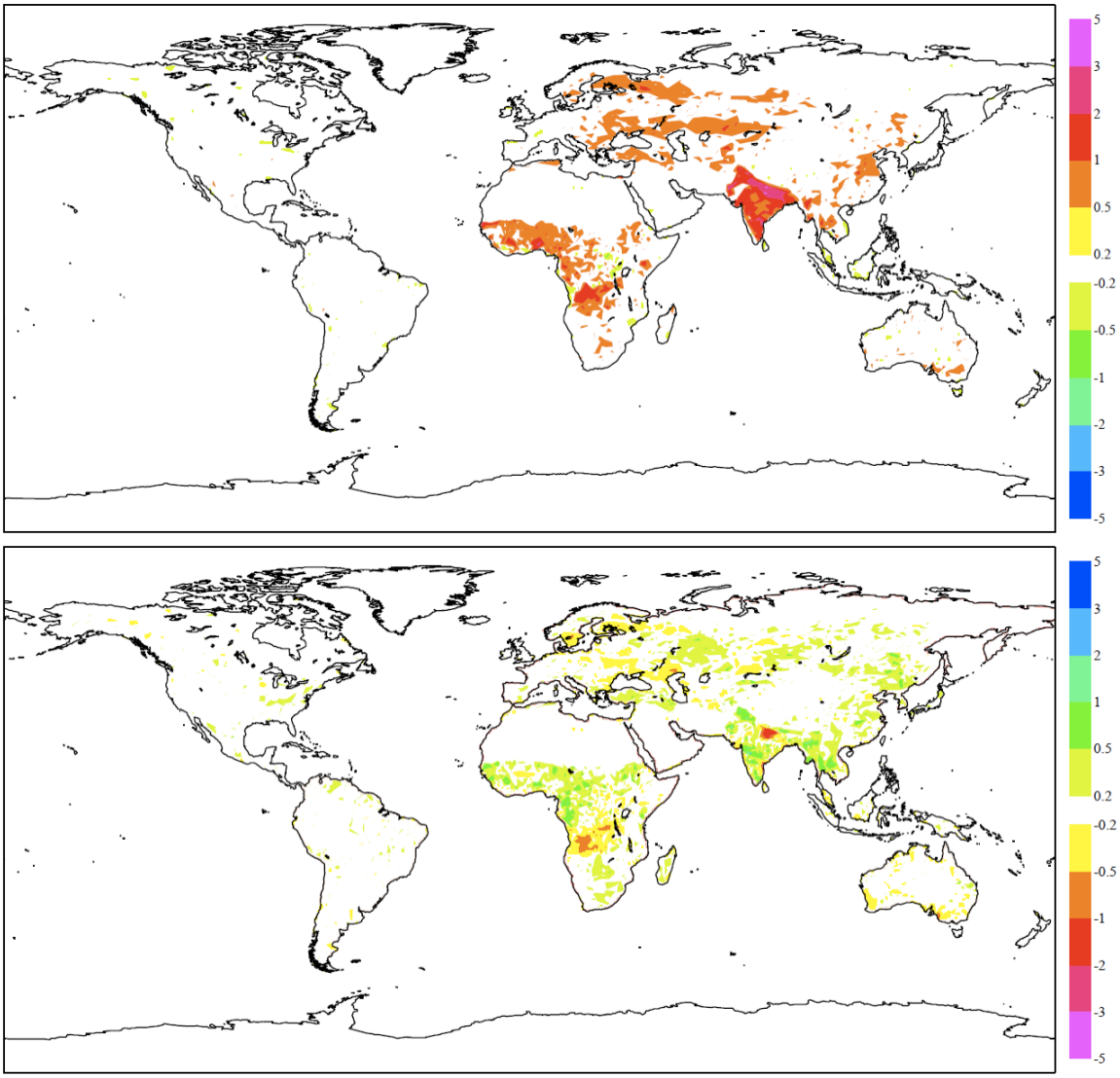

Figure 5: Results from forecast experiments using MODIS LAI relative to the control case for MAM at FC+36 (valid 12UTC), 2m temperature [K]: sensitivity (upper), impact (lower)

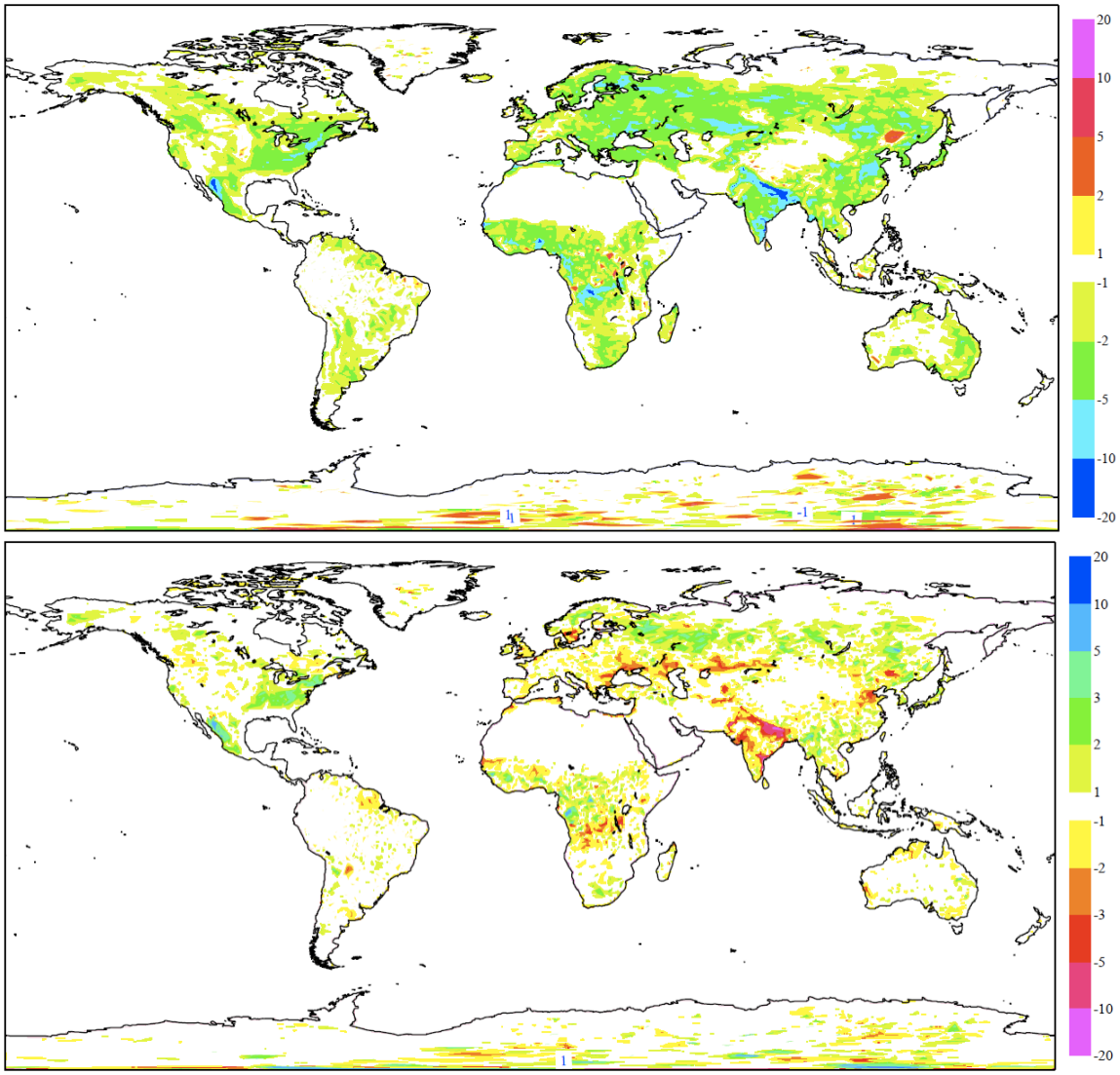

Figure 6: Results from forecast experiments using MODIS LAI relative to the control case for MAM at FC+36 (valid 12UTC), 2m relative humidity[%]: sensitivity (upper), impact (lower)

4.2 Minimum Stomatal resistance adjustment

The current minimum stomatal resistance ($r_{s,\,min}$) values used in HTESSEL were estimated given the fixed LAI look-up table which corresponds to fully developed vegetation throughout the year which generally leads to an $r_{s,\,min}$ bias toward high LAI values. In fact, due to the tight link between the canopy resistance and the LAI (following the Jarvis formulation according to eq. 2), any modification to the LAI would require the adjustment of $r_{s,\,min}$. Actually, when looking at the results of the forecast experiments stratified by vegetation type, we can see that the biases increase for some biomes due to the introduction of the monthly LAI climatology especially in the relative humidity results for crops, grass, needleleaf and broadleaf forest (figure 7). In addition, when comparing the actual look-up table of $r_{s,\,min}$ (table 1) and the literature (Giard and Bazile 2000), a few outliers emerge. Those outliers correspond mainly to the needle-leaf forest and the crops.

Given the little knowledge about $r_{s,\ \min}$, an $r_{s,\ \mathbf{max}} = \frac{r_{s,\ \min}}{LAI_{MAX}}$ was extracted from Giard and Bazile (2000) and compared to the same quantity using the MODIS LAI climatology in order to estimate a new $r_{s,\ \min}$ for the crops and the needle-leaf forest. For the crops, $r_{s,\ \min}$ was changed from 180 to 100 s m^{-1}, and for the needle-leaf forest, it was changed from 500 to 250 while the short grass was given the same value as the tall grass (100). The results show that a change in the minimum stomatal resistance ($r_{s,\ \min}$) was beneficial especially for the 2m relative humidity (table 5) in all seasons without affecting the overall positive impact on the 2m temperature (table 5). This fact is confirmed when stratifying the results by vegetation type as seen in (figure 8) where the impact for crops and needle leaf forest during summer (active evapotranspiration) was improved especially for the relative humidity.

This procedure has potential for improving when generalized through an objective adjustment of the minimum stomatal resistance by minimizing cost-function based on screen-level errors. An ongoing study is dealing with the implementation of this method with the introduction of the near real time LAI observations in order to reduce the vegetation dependent model biases.

Table 5: Sensitivity and impact for MODIS LAI+rs,min, relative to MODIS LAI and control cases for 2m temperature [K] and relative humidity [%] globally over land at FC+36 (valid 12UTC)

Experiment	season	T_sensitivity	T_impact	RH_sensitivity	RH_impact
MODIS LAI + rs,min vs MODIS LAI	DJF	-0.037	-0.002	0.386	0.098
	MAM	-0.072	-0.01	0.643	0.025
	JJA	-0.12	-0.012	0.977	0.158
	SON	-0.056	-0.007	0.625	0.158
MODIS LAI + rs,min vs CTL	DJF	0.091	0.004	-0.579	-0.152
	MAM	0.113	0.025	-0.738	0.002
	JJA	0.057	0.002	-0.225	-0.13
	SON	0.094	0.019	-0.722	-0.13

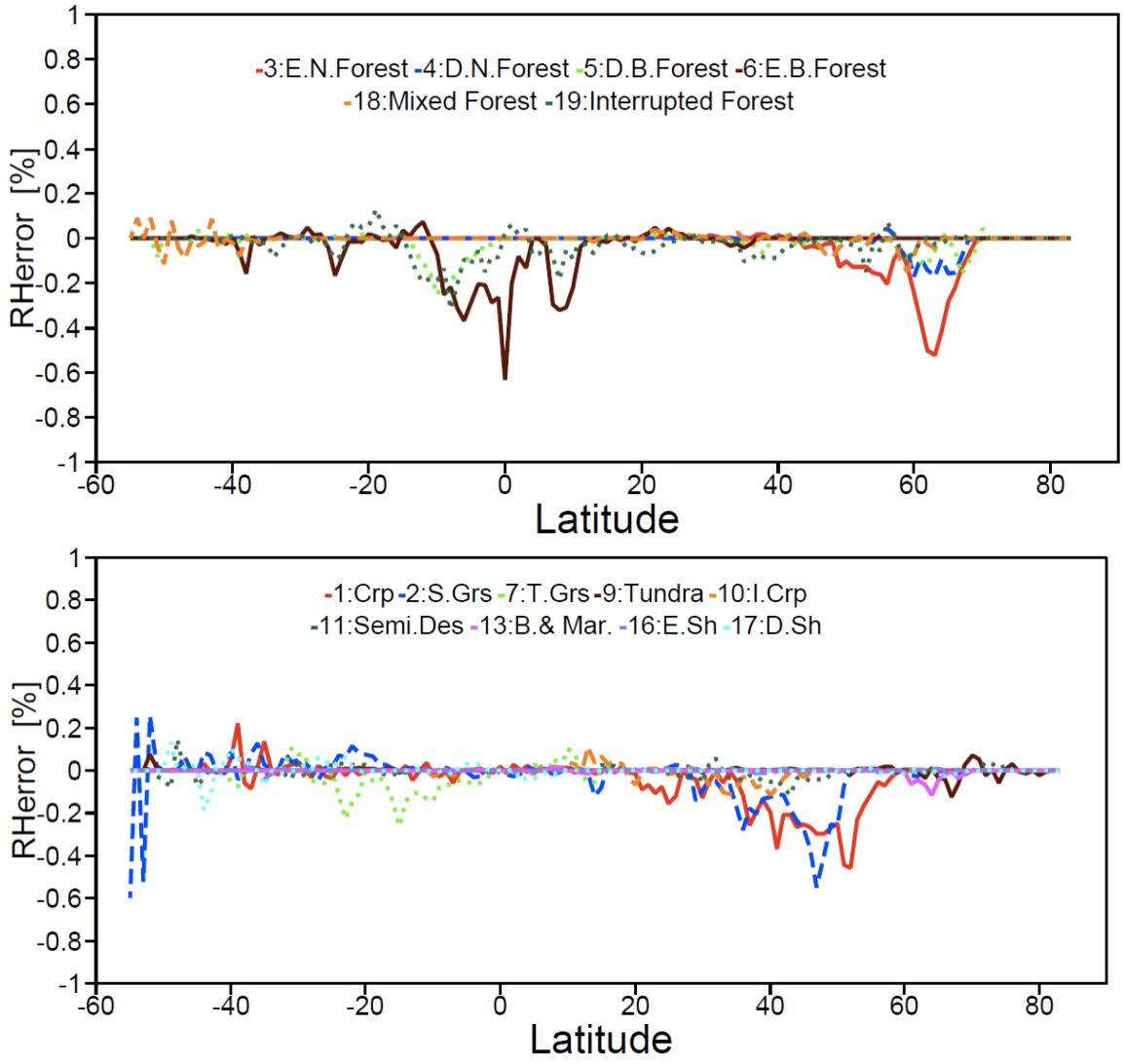

Figure 7: Stratification by vegetation type of the global zonal average impact of (MODIS LAI) on the 2m relative humidity[%] over land in comparison to the (Control) experiment for JJA at FC+36 (valid 12UTC) : (lower) for low vegetation types (crops in red, grass in blue) , (upper) for high vegetation types (evergreen needle-leaf in red, deciduous needle-leaf in blue)

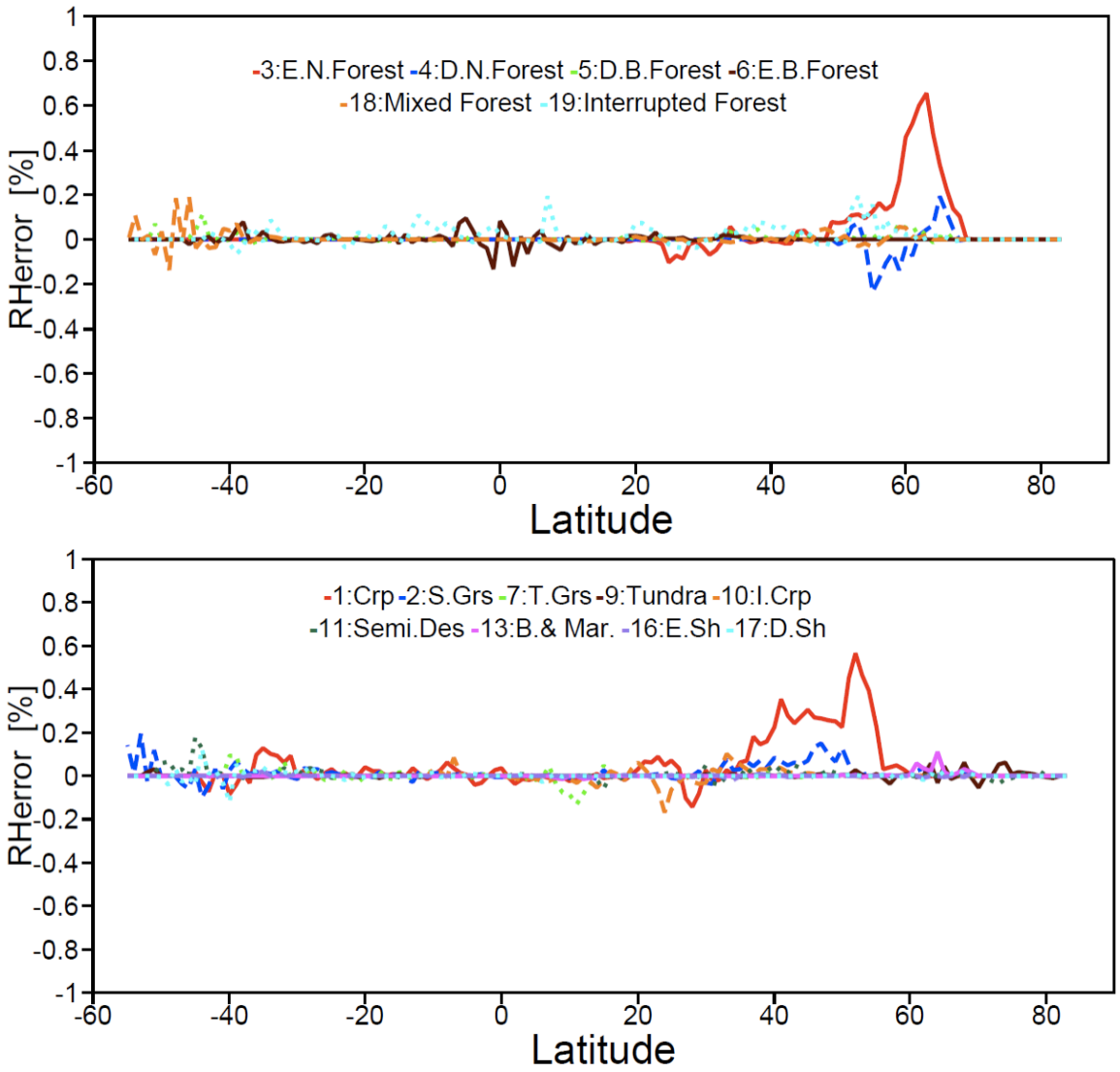

Figure 8: Stratification by vegetation type of the global zonal average impact of rs,min adjustment (MODIS LAI+rs,min) on the 2m relative humidity[%] over land in comparison to the (MODIS LAI) experiment for JJA at FC+36 (valid 12UTC) : (lower) for low vegetation types (crops in red, grass in blue) , (upper) for high vegetation types (evergreen needle-leaf in red, deciduous needle-leaf in blue)

4.3 Assimilation experiments

As seen in section 2, when changing the LAI map, the surface evaporation is affected, and consequently the soil moisture distribution is modified. To allow this new distribution to reach its new equilibrium, long assimilation experiments are required in order to account for surface processes adequate time scale. During an assimilation cycle (12-hour interval in the IFS), we can express the analysis increment δA following the surface water storage (WS) budget (Balsamo et al. 2009):

$$\frac{dWS}{dt} = P + E + R + \delta A \tag{17}$$

Where P is the precipitation, E is the Evaporation, R is the runoff and δA is the analysis increment for snow δs and soil moisture $\delta\theta$. Thus any change in the evaporation could lead to a change in the increments as the analysis makes use of short-term forecast errors in 2-m temperature and relative humidity to correct soil moisture errors via a set of optimal interpolation coefficients (Douville et al. 2000). These assimilation experiments would also allow confirming the effectiveness of the previous one year forecast experiments as a proxy for the assimilation experiments.

Similarly to the forecast experiments, three assimilation experiments were performed from March to August 2008 using respectively the Ctl LAI, ECO-LAI and the MODIS-LAI (table 3). In this case, the same statistics as in the forecast experiment were used with the only exception that for the computation of the impact, instead of comparing to the operational analysis, the comparison was performed against the experiment's own analysis:

$$T_{\text{impact}} = \left|\mathrm{T}_{ctl} - \mathrm{T}_{own\_an}\right| - \left|\mathrm{T}_{MLAI} - \mathrm{T}_{own\_an}\right| \tag{18}$$

For ECOCLIMAP LAI, the results (table 6) show a cooling for MAM and JJA in the global 2m temperature sensitivity with negative impact in MAM and a slight positive one in JJA corresponding to an increase in relative humidity with positive impact in both seasons. In fact, after reaching a new equilibrium between the vegetation transpiration caused by the new LAI distribution and the soil moisture content, the higher summer LAI (figure 4) in ECOCLIMAP cause more transpiration than in the control case. In the MODIS LAI case (table 6), these sensitivities were reversed causing a positive impact for both the 2m temperature and relative humidity in the 2 seasons.

Table 6: Sensitivity and impact for 2m temperature [K] and relative humidity [%] globally over land at FC+36 (valid 12UTC) in Data Assimilation experiments.

Experiment	season	T_sensitivity	T_impact	RH_sensitivity	RH_impact
ECOCLIMAP LAI vs CTL	MAM	-0.0291	-0.0051	0.1911	0.0257
	JJA	-0.0082	0.0018	0.1377	0.0532
MODIS LAI + rs,min vs CTL	MAM	0.0706	0.027	-0.4782	0.0691
	JJA	0.0373	0.0119	-0.1238	0.0174
MODIS LAI + rs,min vs ECOCLIMAP	MAM	0.0997	0.0321	-0.6692	0.0434
	JJA	0.0455	0.0101	-0.2616	-0.0358

In terms of sensitivity, the MODIS LAI assimilation results confirm the results of forecast only experiments (section 4.1) with a warming trend for both MAM and JJA leading to a moisture reduction in both cases. It is worth mentioning that the sensitivity magnitude is smaller in the assimilation experiment. The assimilation system tries to compensate for the loss of evapotranspiration caused by smaller LAI by adding soil moisture as can be seen in (figure 9) where the root zone (top 1m) soil moisture mean increments for JJA are mostly positive. However these increments are smaller than those of the control experiment corresponding to an overall positive impact (figure 10) of 0.3%

on average. This means that given the HTESSEL formulation, the new LAI distribution is improving the surface model performance as it contributes to the improvement of the soil moisture distribution. In addition, these results suggest that the forecast only experiments indicate at least qualitatively the correct impact of seasonal LAI in the full system (which includes data assimilation).

Given that the comparison between the two seasonal LAI results showed that in general MODIS LAI has a better impact on the 2 m temperature and relative humidity than ECOCLIMAP (tables 6 and 11), that the former also includes a multi-year climate, and that MODIS has the potential to be used in real time with perspective for similar follow-on missions, MODIS was chosen for the operational implementation (for the IFS cycle 36R4 the 7th of November 2010).

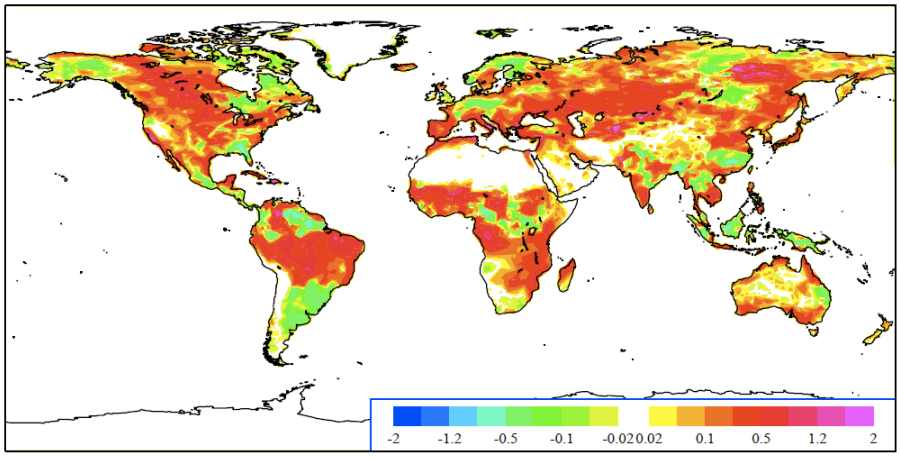

Figure 9: Mean top 1m Soil moisture analysis increments [mm/day] for JJA as computed using MODIS LAI+rs,min

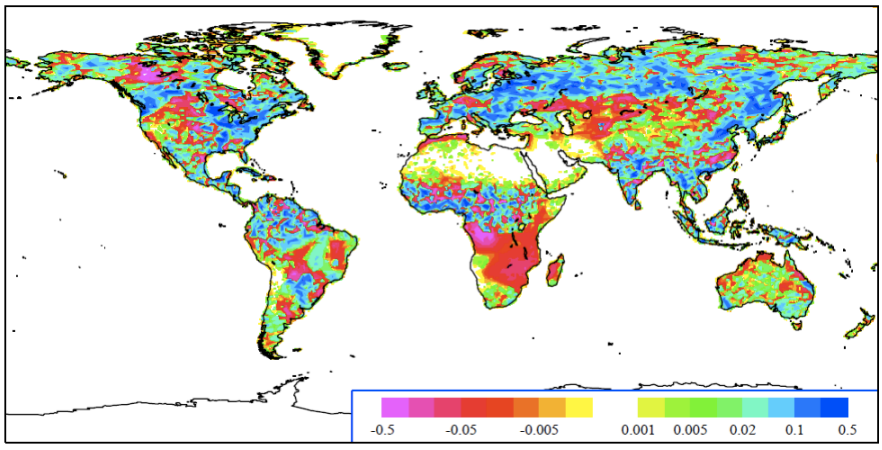

Figure 10: Impact on mean top 1m Soil moisture analysis increments [mm/day] for JJA comparing the MODIS LAI+rs,min case to the control (|Control-LAI increments|-|MODIS-LAI increments|)

4.4 Long integration experiments

Focusing on the land surface seasonal time scale, ensembles of multi-month long integrations, referred to as climate simulations have been performed, using a model configuration with 91 vertical layers and a gridpoint resolution of about 120 km (spectral truncation T159). They consisted of 13-month long 4-member ensemble hindcasts (with observed SSTs) covering the period from 01/08/2000 to 31/08/2001. Two sets of simulations were performed: (i) with the control LAI and (ii) the MODIS LAI climatology. A positive impact is seen in temperature at 2m compared with ERA-Interim climatology as shown in figure 11.

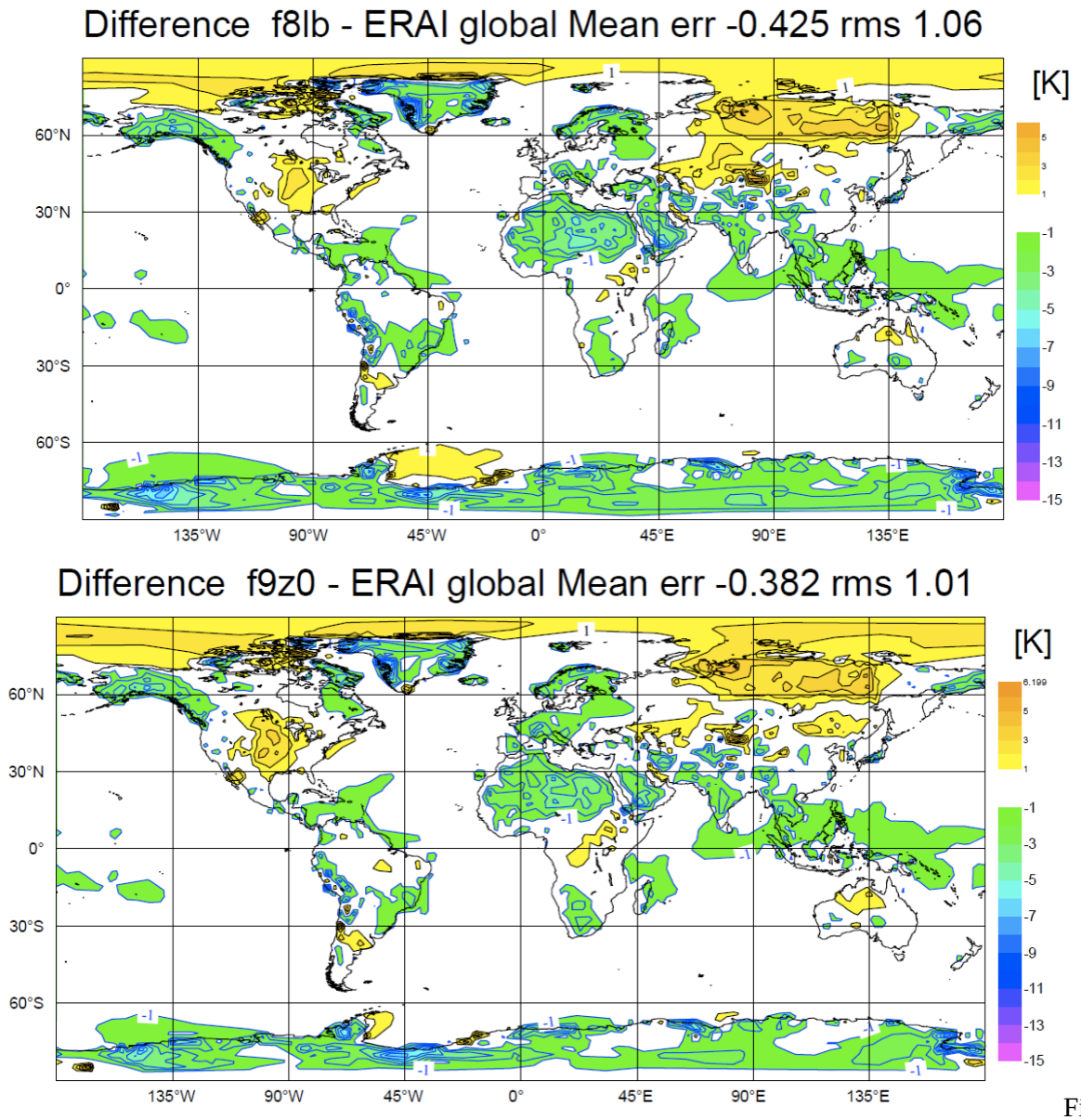

Figure 11: *Annual mean 2m temperature error [K] of the model climate (compared to ERA-Interim) for the CONTROL (upper) and MODIS LAI+rs,min,(lower).*

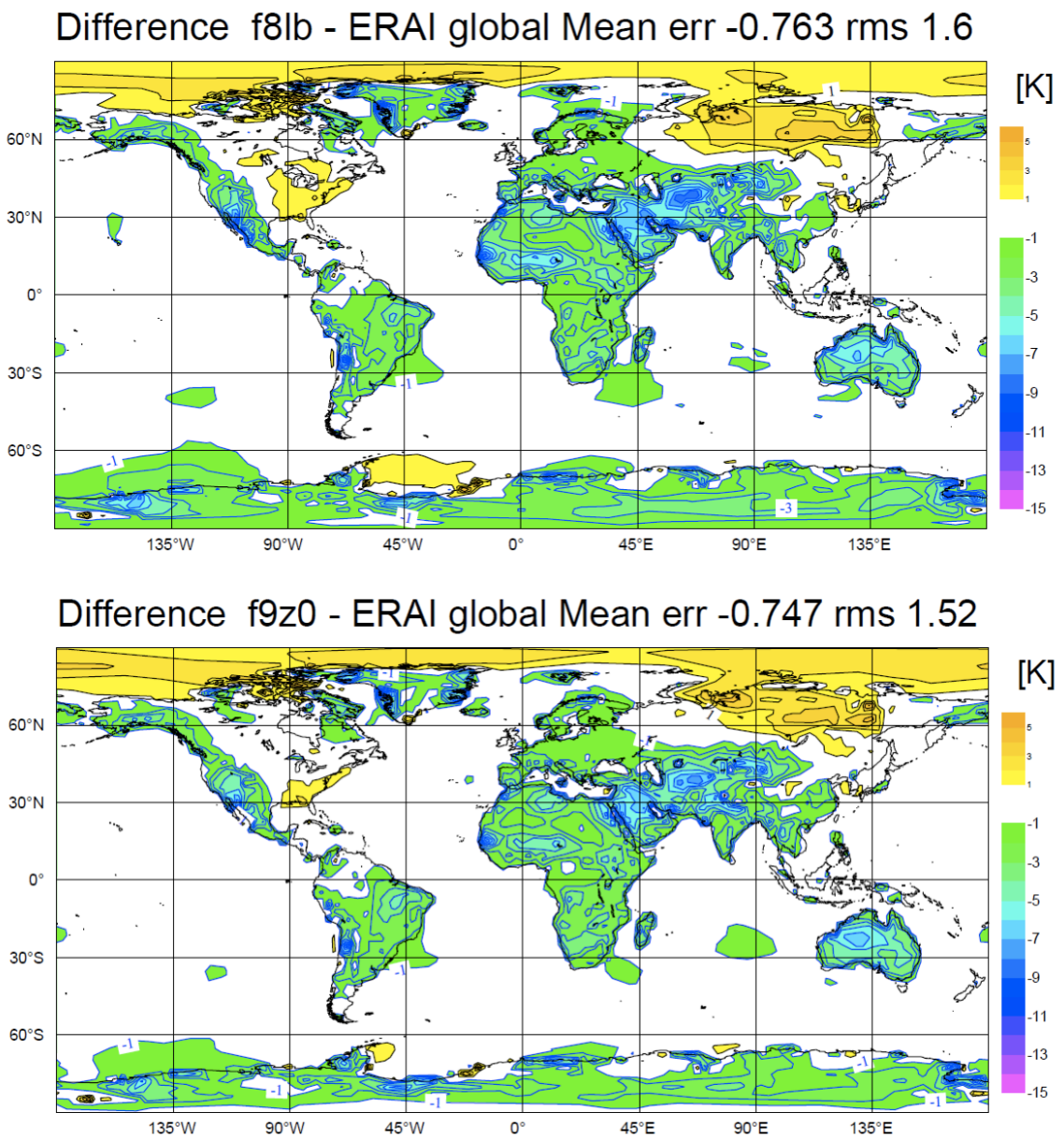

Figure 12: Annual mean 2m dew point error [K] of the model climate (compared to ERA-Interim) for the CONTROL (upper) and MODIS LAI+rs,min,(lower).

The 2m temperature annual RMSE error (based on monthly averages) is reduced from 1.06 K to 1.01K, while the 2m dew-point temperature error is reduced from 1.60 K to 1.52 K (figure 12). Verification of the surface wind over the ocean using satellite observations from SSMI and QUIKSCAT shows that the 10m wind bias is improved by about 5%, indicating that the new LAI distribution is affecting the large scale flow through the surface fluxes over land. Inline with these errors reductions, the atmospheric water and vapour contents showed also an improvement as a result of better surface fluxes and wind fields distribution.

In fact, the total cloud liquid water bias is also improved by 5% compared to the TRMM product and by 1% compared to the SSMI product and the total column water vapour and integrated water show a bias reduction of about 5% compared to the SSMI and NOAA products respectively. This confirms

that overall, the model climate (surface and upper-air) is improved or neutral when the MODIS based monthly LAI climatology is introduced.

5 Discussion and summary

Owing to the importance of the vegetation in the land-atmosphere interaction processes, numerous studies have tried to use the satellite observations to give information on the vegetation layer, and attempted to evaluate the quality of this information through their signals and impacts. This study assesses two satellite derived monthly LAI climatology datasets and their meteorological impact as opposed to a vegetation dependent LAI constant throughout the year.

Based on the analysis of the two satellites derived climatologies, their spatial distribution, and patterns are discussed. Both ECOCLIMAP and MODIS LAI climatologies have similar global spatial signatures, nevertheless, the magnitude and the spatial extent of these signatures can vary significantly by regions. In addition, a larger seasonal variability is expressed in ECOCLIMAP than in MODIS products especially in the northern hemisphere and obviously neglected in the fixed map. Sensor differences, retrieval algorithms, and atmospheric correction methods have been hypothesised as major reasons for these discrepancies. This intrinsic comparison does not allow identifying which product is better. The assessment of the impact of these two observation based climatologies on the near surface atmosphere was then done as an alternative to distiguish which product is more suitable to be used within the IFS.

Three types of global model experiments (medium range forecasts, data assimilation experiments and long integrations to study the climate of the model) were performed using the ECMWF IFS-HTESSEL system. Results show an overall positive impact on the model climate with marked improvement in transitional seasons (spring/fall). Extensive data assimilation and forecasts experiments confirm the benefit coming from a more realistic treatment of vegetation LAI in near surface weather parameters. Future research will consider the use of MODIS products in a data assimilation system in order to account for near real time issues such us a rapid change in the LAI due to fast growth or harvest as well as interannual variability due for instance to an extreme drought or an extensive snow season that may inihibit growth. The new implementation of an Extended Kalman filter-based surface data assimilation within the IFS would be a suitable framework for such study. The verification will then be extended to a larger number of instrumented sites in order to investigate vegetation dependent model biases. Such observartions could be used for an objective optimization of the minimum stomatal resistance assuming that the assimilated soil moisture within the IFS system is of good quality.

Acknowledgements

We would like to thank Alan Betts and Tilden Meyers for their valuable comments on the results. Testing for a monthly LAI has been initiated by Bart van den Hurk and Martijn Brandt at KNMI and we acknowledge their effort. We would like to thank Philippe Lopez, Peter Bechtold, Deborah Salmond and Jan Haseler for help during the testing and implementation phases. This work is a

contribution to the GEOLAND-2 project, funded by the European Commission within the GMES initiative in FP7.

References

Avissar, R., and Y. Liu, 1996, Three-dimensional numerical study of shallow convective clouds and precipitation induced by land surface forcing. Journal of Geophysical Research, 101, 7499 −7518.

Balsamo G., P. Viterbo, A.C.M. Beljaars, B. van den Hurk, M. Hirchi, A. Betts, and K. Scipal, 2009, A revised hydrology for the ECMWF model: Verification from field site to terrestrial water storage and impact in the integrated forecast system. Journal of Hydrometeorology 10, 623-643.

Baret F., O. Hagolle, B. Geiger, P. Bicheron, B. Miras, M. Huc, B. Berthelot, F. Niño, M. Weiss, O. Samain, J.L. Roujean and M. Leroy, 2007, LAI, fAPAR and fCover CYCLOPES global products derived from VEGETATION: Part 1: Principles of the algorithm. Remote Sensing of Environment, 110, 275-286.

Betts A.K., J. H. Ball, A.C.M Beljaars, M.J. Miller, and P.A. Viterbo, 1996, The land-surface-atmosphere interaction: A review based on observational and global modelling perspective. Journal of Geophysical Research, 101, 7209-7225.

Boussetta, S., T. Koike, Y. Kun, T. Graf, and M. Pathmathevan, 2008, Developement of a coupled land-atmosphere satellite data assimilation system for improved local atmospheric simulations. Remote Sensing of Environment, 112, 720-734.

Garrigues S., R. Lacaze, F. Baret, J. T. Morisette, M. Weiss, J. E. Nickeson, R. Fernandes, S. Plummer, N. V. Shabanov, R. B. Myneni, Y. Knyazikhin, and W. Yang, 2008, Validation and intercomparison of global Leaf Area Index products derived from remote sensing data. Journal of Geophysical Research, 113, G02028, doi:10.1029/2007JG000635.

Deardorff, J.W., 1978, Efficient prediction of ground surface temperature and moisture, with inclusion of a layer of vegetation. Journal of Geophysical Research, 83, 1889-1903.

Dickinson, R., A. Henderson-Sellers, and P. Kennedy, 1993, Biosphere-Atmosphere Transfer Scheme (BATS) version 1e as coupled to the NCAR community climate model. Technical Report NCAR/TN-387 + STR, NCAR Boulder, Colorado.

Dorman J.L. and P. J. Sellers, 1989, A Global Climatology of Albedo, Roughness Length and Stomatal Resistance for Atmospheric General Circulation Models as Represented by the Simple Biosphere Model (SiB). Journal of Applied Meteorology, 28, 833-855.

Douville H., P. Viterbo, J.-F. Mahfouf, and A.C.M. Beljaars, 2000, Evaluation of the optimum interpolation and nudging techniques for soil moisture analysis using FIFE data. Monthly Weather Review, 128, 1733-1756.

Giard D. and E. Bazile, 2000, Implementation of a new assimilation scheme for soil and surface variables in a Global NWP model. Monthly Weather Review, 128, 997-1015.

Guillevic, P., R. D. Koster, M.J. Suarez, L. Bounoua, G.J. Collatz, S.O. Los, and S.P.P.Mahanama, 2002, Influence of the interannual variability of vegetation on the surface energy balance - a global sensitivity study. Journal of Hydrometeorology, 3, 617-629.

Jacobs, C.M.J. and H.A.R. DE Bruin, 1992, The Sensitivity of regional transpiration to land-surface characteristics - significance of feedback. Journal of Climate 60, 683-698.

Jarlan, L., G. Balsamo, S. Lafont, A.C.M. Beljaars, J.-C. Calvet and E. Mougin, 2008, Analysis of Leaf Area Index in the ECMWF land surface scheme and impact on latent heat and carbon fluxes: Applications to West Africa, Journal of Geophysical Research, 113, D24117, doi: 10.1029/2007JD009370.

Jarvis, P. J., 1976, The interpretation of the variations in leaf-water potential and stomatal conductance found in canopies in the field, Philosophical Transaction of the Royal Society London, B723, 385-610.

Kanemasu, T., U.D. Rosenthal, R.J. Stone and L.R. Stone, 1977, Evaluation of an evapotranspiration model of corn. Journal of Agronomy, 69, 461-464.

Knote, C., G. Bonafe and F. DI Guiseppe, 2009, Leaf Area Index Specification for Use in Mesoscale Weather Prediction Systems. Monthly Weather Review, 137, 3535-3550

Knyazikhin, Y., J.V. Martonchik, R.B. Myneni, D.J. Diner, and S.W. Running, 1998, Synergistic algorithm for estimating vegetation canopy leaf area index and fraction of absorbed photosynthetically active radiation from MODIS and MISR data, Journal of Geophysical Research, 103, 32257-32276.

Koster, R. D., S. Mahanama, T. Yamada, G. Balsamo, M. Boisserie, P. Dirmeyer, F. Doblas-Reyes, T. Gordon, Z. Guo, J.-H. Jeong, D. Lawrence, Z. Li, L. Luo, S. Malyshev, W. Merryfield, S. I. Seneviratne, T. Stanelle, B. van den Hurk, F. Vitart, E. F. Wood, 2009, The Contribution of Land Surface Initialization to Subseasonal Forecast Skill: First Results from the GLACE-2 Project, Geophysical Research Letters, 2009GL041677R.

Lawrence D. M. and J.M. Slingo, 2004, An annual cycle of vegetation in a GCM. Part I: implementation and impact on evaporation, Climate Dynamics, 22, 87-105.

Los, S.O., G.J. Collatz, P.J. Sellers, C.M. Malmström, N.H. Pollack, R.S. DeFries, L. Bounoua, M.T. Parris, C.J. Tucker, and D.A. Dazlich, 2000, A global 9-year biophysical land-surface dataset from NOAA AVHRR data, Journal of Hydrometeorology, 1, 183-199.

Lotsch, A., Y. Tian, M.A. Friedl, and R.B. Myneni, 2003, Land cover mapping in support of LAI and FPAR retrievals from EOS-MODIS and MISR: classification methods and sensitivities to errors. International Journal of Remote Sensing, 24, 1997-2016.

Loveland, T. R., B.C. Reed, J.F. Brown, D.O. Ohlen, Z. Zhu, L. Youing, and J.W. Merchant, 2000: Development of a global land cover characteristics database and IGB6 DISCover from the 1km AVHRR data. International Journal of Remote Sensing, 21, 1303–1330.

Masson, V., J.L. Champeaux, F. Chauvin, C. Meriguet, and R. Lacaze, 2003 : A global database of land surface parameters at 1-km resolution in meteorological and climate models, Journal of Climate, 16, 1261-1282.

Myneni, R. B. et al., 2002. Global products of vegetation leaf area and fraction absorbed PAR from year one of MODIS data. Remote Sensing of Environment, 83, 214-231.

Sellers, P.J., Y. Mintz, Y.C. Sud and A. Dalcher, 1986. A simple biosphere model (SiB) for use within general circulation models. Journal of Atmospheric Science, 43, 505-531.

Sellers, P.J., S.O. Los, C.J. Tucker, C.O. Justice, D.A. Dazlich, G.J. Collatz and D.A. Randall, 1996: A revised land surface parameterization (SiB2) for atmospheric GCMs, Part II: The generation of global fields of terrestrial biophysical parameters from satellite data. Journal of Climate, 9, 676–705.

Viterbo, P., and A.C.M. Beljaars, 1995: An improved land surface parametrization scheme in the ECMWF model and its validation. Journal of Climate, 8, 2716-2748.

Van den Hurk, B., P. Viterbo, A. Beljaars, and A.K. Betts, 2000: Offline validation of the ERA-40 surface scheme, ECMWF Tech. Memo. No. 295.

Van den Hurk, B., P. Viterbo, and S. Los, 2003: Impact of leaf area index seasonality on the annual land surface evaporation in a global circulation model. Journal of Geophysical Research, 108, D6, 4191, doi:10.1029/2002JD002846.

Wilson T.B. and T.P. Meyers, 2007: Determining vegetation indices from solar and photosythetically active radiation fluxes. Agriculture and Forest Meteorology 144, 160-179.